

Static Magnetization of V_{15} Cluster at Ultra-Low Temperatures: Precise Estimation of Antisymmetric Exchange

Alex Tarantul,[†] Boris Tsukerblat,^{*,†} and Achim Müller[‡]

Department of Chemistry, Ben-Gurion University of the Negev, 84105 Beer-Sheva, Israel, and
Fakultät für Chemie, Universität Bielefeld, 33501 Bielefeld, Germany

Received July 26, 2006

In this article, the low-temperature static (adiabatic) magnetization data of the nanoscopic V_{15} cluster present in $K_6[V^{IV}_{15}As_6O_{42}(H_2O)] \cdot 8H_2O$ is analyzed. The cluster anion, which attracted much attention in the past, contains a triangular V^{IV}_3 array causing frustration as a function of applied field and temperature. In the analysis, a three-spin ($S = 1/2$) model of V_{15} was employed that includes isotropic antiferromagnetic exchange interaction and antisymmetric (AS) exchange in the most general form compatible with the trigonal symmetry of the system. It was shown that, along with the absolute value of AS exchange, the orientation of the AS vector plays a significant physical role in spin-frustrated systems. In this context, the role of the different components of the AS in the low-temperature magnetic behavior of V_{15} was analyzed, and we were able to reach a perfect fit to the experimental data on the staircaselike dependence of magnetization versus field in the whole temperature range including extremely low temperature. Furthermore, it was possible for the first time to precisely estimate the two components of the AS vector coupling constant in a triangular unit, namely, the effective in-plane component, D_L , and the perpendicular part, D_n .

1. Introduction

The cluster anion present in $K_6[V^{IV}_{15}As_6O_{42}(H_2O)] \cdot 8H_2O$ (V_{15} cluster) was discovered more than 15 years ago.¹ Since that time this system has attracted continuous and increasing attention as a *unique* molecular magnet based on an *unique* structure exhibiting layers of different magnetization.^{2–4} The V_{15} cluster became an interesting subject of nanoscopic physics and chemistry (see recent book⁵ that exhaustively covers this fascinating area of molecular magnetism). Studies of the static (adiabatic) magnetization and quantum dynamics of the V_{15} cluster which can, despite the low $S = 1/2$ ground state, be considered as a mesoscopic system, proved that the system exhibits the hysteresis loop of magnetization of molecular origin.^{5–11} The magnetic properties of the V_{15}

cluster are inherently related to the spin-frustration effect in the layered but quasispherical arrangement of vanadium ions, and from this point of view, it represents a system for which the manifestations of the antisymmetric (AS) exchange interaction, introduced by Dzyaloshinsky¹² and Moria,¹³ are especially interesting. The understanding of the special role of the AS exchange in spin-frustrated systems, particularly in trinuclear transition metal clusters, dates back to the seventies (see review article¹⁴ and references therein). The AS exchange was shown to result in a zero-field splitting of the frustrated ground state of the half-integer triangular spin systems, magnetic anisotropy, essential peculiarities of the EPR spectra, and a wide range of phenomena related to hyperfine interactions.^{14–26} Recently, large AS exchange was evoked by Solomon and co-workers²⁷ to interpret the unusual properties of tricopper clusters. On the contrary, other forms

* To whom correspondence should be addressed. E-mail: tsuker@bgu.ac.il.

[†] Ben-Gurion University of the Negev.

[‡] Universität Bielefeld.

- (1) Müller, A.; Döring, J. *Angew. Chem., Int. Ed. Engl.* **1988**, *27*, 1721.
- (2) Gatteschi, D.; Pardi, L.; Barra, A.-L.; Müller, A.; Döring, J. *Nature* **1991**, *354*, 465.
- (3) Barra, A.-L.; Gatteschi, D.; Pardi, L.; Müller, A.; Döring, J. *J. Am. Chem. Soc.* **1992**, *114*, 8509.
- (4) Gatteschi, D.; Pardi, L.; Barra, A.-L.; Müller, A. *Mol. Eng.* **1993**, *3*, 157.
- (5) Gatteschi, D.; Sessoli, R.; Villain, J. *Molecular Nanomagnets*; Oxford University Press: Oxford, U.K., 2006.
- (6) Barbara, B. *J. Mol. Struct.* **2003**, *656*, 135.
- (7) Chiorescu, I.; Wernsdorfer, W.; Müller, A.; Bögge, H.; Barbara, B. *Phys. Rev. Lett.* **2000**, *84*, 3454.

- (8) Chiorescu, I.; Wernsdorfer, W.; Müller, A.; Miyashita, S.; Barbara, B. *Phys. Rev. B* **2003**, *67*, 020402(R).
- (9) Miyashita, S. *J. Phys. Soc. Jpn.* **1996**, *65*, 2734.
- (10) Nojiri, H.; Taniguchia, T.; Ajiro, Y.; Müller, A.; Barbara, B. *Physica B* **2004**, *346–34*, 216.
- (11) Miyashita, S. *J. Phys. Soc. Jpn.* **1995**, *64*, 3207.
- (12) Dzyaloshinsky, I. *E. Zh. Exp. Teor. Fiz.* **1957**, *32*, 1547; *Sov. Phys. JETP* **1957**, *5*, 1259.
- (13) Moria, T. *Phys. Rev.* **1960**, *120*, 91.
- (14) Tsukerblat, B. S.; Belinskii, M. I.; Fainzilberg, V. E. *Magnetochemistry and spectroscopy of transition metal exchange clusters*. In *Soviet Science Review B*; Vol'pin, M., Ed.; Harwood Academic: Yverdon, Switzerland, 1987; pp 337–482.

of the non-Heisenberg interactions have a secondary importance in the case under consideration. For instance, the biquadratic exchange is not operative in $S = 1/2$ systems, and the symmetric anisotropic forms of the exchange tensor act as second-order perturbations.

In this article, we focus on the three-spin ($S = 1/2$) model^{3–5} that takes into account isotropic and AS exchange interactions²⁸ and the axial type of Zeeman interaction for the study of the low-lying spin excitations in the V_{15} cluster. We analyze the energy pattern of the system and deduce simple and accurate approximate expressions for the energy levels in different ranges of the field. Then, it is shown how the different components of the AS exchange affect the field dependence of magnetization of the V_{15} cluster at low temperatures. Finally, we apply the theoretical model to the analysis of the experimental data²⁹ on the magnetization of V_{15} versus field at ultralow temperature and show that the model provides a perfect fit to the experimental data in the whole range of the applied fields and temperatures. It has been concluded that the AS exchange interaction is crucially important for understanding the observed shape of the staircaselike field dependence of magnetization of the V_{15} cluster at low temperatures. Analyzing the experimental data, we were able to determine precisely two independent parameters of the AS exchange. In a more wide sense, the results of this study are related to an important issue of molecular magnetism focused on the study of the magnetic anisotropy^{30–33} and mechanisms of quantum tunneling of magnetization in multispin systems.⁵ The present study is considered to be part of a more extended futural investigation

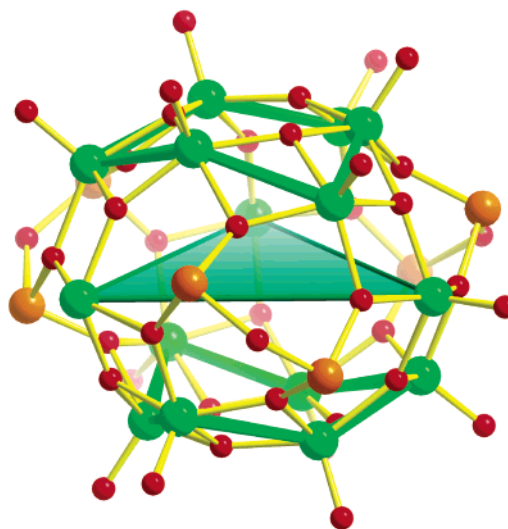


Figure 1. The cluster anion $[V^{IV}_{15}As_6O_{42}(H_2O)]^{6-} = \{V_{15}As_6\}$ (in ball-and-stick representation) without the central water molecule emphasizing the V_3 triangle (transparent green), defined by a crystallographic C_3 axis: V, green; As, orange; O, red. The outer V_6 hexagons are highlighted by thick green lines.

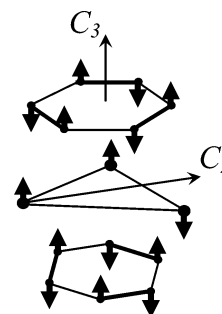


Figure 2. Scheme of the V_{15} metal network and spin arrangement in the low-energy region.

regarding structure-related magnetism of giant polyoxometalates/vanadates showing frustration from one-triangle (present paper) via two- (for M_6Mo_{57} ^{34a}) to 20-triangle spin arrays (for $M_{30}Mo_{72}$, $M = V^{IV}$, Fe^{III} ^{34b}).

2. The Model, AS Exchange

The molecular cluster V_{15} has a distinctly layered quasi-spherical structure within which fifteen V^{IV} ions ($s_i = 1/2$) are placed in an arrangement of a central triangle sandwiched by two hexagons.^{1,2} In Figure 1, the overall structure of V_{15} is illustrated, which at low temperatures consists of two hexanuclear V^{IV}_6 spin-paired systems with a frustrated V^{IV}_3 triangle between them, resulting in an $S = 1/2$ ground state of the entire system (Figure 2). The model of a spin triangle (three-spin model) proposed and substantiated by Gatteschi et al. on the basis of the exact diagonalization of the 15-spin exchange Hamiltonian,^{3,4} gives accurate and descriptive results for the low-lying set of levels and allows adequate discussion of the system behavior at low temperatures ($T < 20$ K) when the spins of the hexagons are paired. The

- (15) Belinskii, M. I.; Tsukerblat, B. S.; Ablov, A. V. *Phys. Status Solidi* **1972**, K71.
- (16) Belinskii, M. I.; Tsukerblat, B. S. *Fiz. Tverdogo Tela* (Russian) **1973**, 15, 29.
- (17) Tsukerblat, B. S.; Belinskii, M. I.; Ablov, A. V. *Fiz. Tverdogo Tela* (Russian) **1974**, 16, 989.
- (18) Tsukerblat, B. S.; Belinskii, M. I. *Magnetochemistry and Radiospectroscopy of Exchange Clusters* (Russian); Stiintska: Kishinev, Russia, 1983.
- (19) Tsukerblat, B. S.; Kuyavskaya, B. Ya.; Belinskii, M. I.; Ablov, A. V.; Novotortsev, V. M.; Kalinnikov, V. T. *Theor. Chim. Acta* **1975**, 38, 131.
- (20) Belinskii, M. I.; Tsukerblat, B. S.; Ablov, A. V. *Mol. Phys.* **1974**, 28, 283.
- (21) Tsukerblat, B. S.; Fainzilberg, V. E.; Belinskii, M. I.; Kuyavskaya, B. Ya. *Chem. Phys. Lett.* **1983**, 98, 149.
- (22) Tsukerblat, B. S.; Kuyavskaya, B. Ya.; Fainzilberg, V. E.; Belinskii, M. I. *Chem. Phys.* **1984**, 90, 361; **1984**, 90, 373.
- (23) Fainzilberg, V. E.; Belinskii, M. I.; Kuyavskaya, B. Ya.; Tsukerblat, B. S. *Mol. Phys.* **1985**, 54, 799.
- (24) Tsukerblat, B. S.; Botsan, I. G.; Belinskii, M. I.; Fainzilberg, V. E. *Mol. Phys.* **1985**, 54, 813.
- (25) Fainzilberg, V. E.; Belinskii, M. I.; Tsukerblat, B. S. *Solid State Commun.* **1980**, 36, 639.
- (26) Fainzilberg, V. E.; Belinskii, M. I.; Tsukerblat, B. S. *Mol. Phys.* **1981**, 44, 1177; **1981**, 44, 1195; **1982**, 45, 807.
- (27) Yoon, J.; Mirica, L. M.; Stack, T. D. P.; Solomon, E. I. *J. Am. Chem. Soc.* **2004**, 126, 12586.
- (28) Tsukerblat, B.; Tarantul, A.; Müller, A. *Phys. Lett. A* **2006**, 353, 48.
- (29) Chiorescu, I.; Wernsdorfer, W.; Müller, A.; Bögge, H.; Barbara, B. J. *Magn. Magn. Mater.* **2000**, 221, 103.
- (30) Tsukerblat, B. S.; Palii, A. V.; Ostrovsky, S. M.; Kunitsky, S. V.; Klokishner, S. I.; Dunbar, K. R. *J. Chem. Theory Comput.* **2005**, 1, 668.
- (31) Boča, R. *Coord. Chem. Rev.* **1998**, 173, 167.
- (32) Boča, R. *Coord. Chem. Rev.* **2004**, 248, 757.
- (33) Boča, R. *Theoretical Foundations of Molecular Magnetism*; Elsevier: Amsterdam, 1999.

- (34) (a) Gatteschi, D.; Sessoli, R.; Plass, W.; Müller, A.; Krickemeyer, E.; Meyer, J.; Sölter, D.; Adler, P. *Inorg. Chem.* **1996**, 35, 1926 and references therein. (b) Müller, A.; Todea, A. M.; van Slageren, J.; Dressel, M.; Bögge, H.; Schmidtman, M.; Luban, M.; Engelhardt, L.; Rusu, M. *Angew. Chem., Int. Ed.* **2005**, 44, 3857 and references therein.

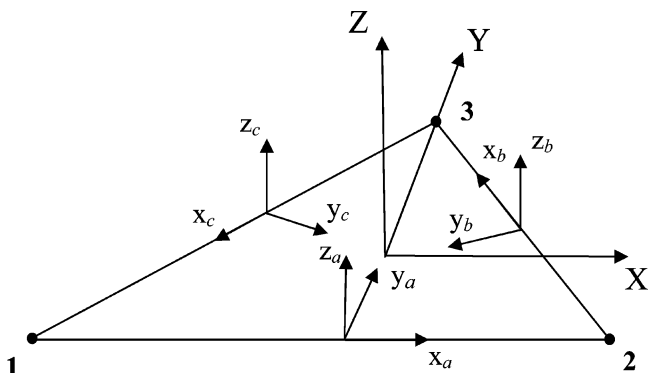


Figure 3. Local $(x_i y_i z_i)$ and molecular (XYZ) coordinate systems for the vanadium triangle in V_{15} .

isotropic superexchange can be described by the conventional HDVV Hamiltonian for a triangular cluster

$$H_0 = -2J_0(\mathbf{S}_1\mathbf{S}_2 + \mathbf{S}_2\mathbf{S}_3 + \mathbf{S}_3\mathbf{S}_1) \quad (1)$$

with $S_i = 1/2$ and J_0 being the parameter of the antiferromagnetic exchange ($J_0 < 0$); we will use a positive parameter $J = -J_0$, and the spin functions will be labeled as $|S_1 S_2 (S_{12}) S_3 SM\rangle \equiv |(S_{12}) SM\rangle$. The energy pattern $\epsilon_0(S) = J[S(S+1) - 9/4]$ includes two degenerate spin doublets with $\epsilon_0(1/2) = -(3/2)J$ and a spin quadruplet with $\epsilon_0(3/2) = (3/2)J$ separated by the gap $3J$. This gap can be estimated approximately as 2.6 cm^{-1} , while the remaining levels that are associated with the spin excitations in the hexagons are found at least 500 cm^{-1} above, that justifies the three-spin model so far discussed.

The three vectors \mathbf{D}_{ij} ($ij = 12, 23, 31$) of the AS exchange interaction associated with the sides ij of the triangle can be expressed as

$$\mathbf{D}_{ij} = D_l \mathbf{x}_{ij} + D_t \mathbf{y}_{ij} + D_n \mathbf{z}_{ij} \quad (2)$$

where \mathbf{x}_{ij} and \mathbf{y}_{ij} are the unit vectors along and perpendicular to the sides (in plane of the triangle) and \mathbf{z}_{ij} is perpendicular to the plane; these vectors are related to local frames $(a, b, \text{ and } c)$ as shown in Figure 3. The Hamiltonian of AS exchange that is invariant in trigonal symmetry can be represented in the molecular frame as²⁸

$$H_{AS} = D_n([\mathbf{S}_1 \times \mathbf{S}_2]_Z + [\mathbf{S}_2 \times \mathbf{S}_3]_Z + [\mathbf{S}_3 \times \mathbf{S}_1]_Z) + D_l \left([\mathbf{S}_1 \times \mathbf{S}_2]_X - \frac{1}{2} [\mathbf{S}_2 \times \mathbf{S}_3]_X + \frac{\sqrt{3}}{2} [\mathbf{S}_2 \times \mathbf{S}_3]_Y - \frac{1}{2} [\mathbf{S}_3 \times \mathbf{S}_1]_X - \frac{\sqrt{3}}{2} [\mathbf{S}_3 \times \mathbf{S}_1]_Y \right) + D_t \left([\mathbf{S}_1 \times \mathbf{S}_2]_Y - \frac{\sqrt{3}}{2} [\mathbf{S}_2 \times \mathbf{S}_3]_X - \frac{1}{2} [\mathbf{S}_2 \times \mathbf{S}_3]_Y + \frac{\sqrt{3}}{2} [\mathbf{S}_3 \times \mathbf{S}_1]_X - \frac{1}{2} [\mathbf{S}_3 \times \mathbf{S}_1]_Y \right) \quad (3)$$

Here, $[\mathbf{S}_i \times \mathbf{S}_j]$ are the vector products of spin operators, and the parameter D_n is associated with the “normal” component of AS exchange, D_l and D_t are those for the in-plane contributions.

The analysis of the HDVV Hamiltonian (see review article)¹⁴ revealed that the “degeneracy doubling” (i.e., accidental degeneracy) in the ground spin-frustrated state $(S_{12})S = (0)1/2, (1)1/2$ is related to the exact orbital degeneracy so that the ground term is the orbital doublet 2E of a trigonal point group. It was concluded¹⁴ that the AS

exchange acts within the $(S_{12})S = (0)1/2, (1)1/2$ manifold like a first-order spin-orbital interaction within the 2E term and gives rise to two Kramers doublets in agreement with Kramers theorem. The matrix of the full Hamiltonian $H_0 + H_{AS}$ including the axial Zeeman interaction

$$H_{\text{Zeem}} = g_{\parallel} \beta H_Z S_Z + g_{\perp} \beta (H_X S_X + H_Y S_Y) \quad (4)$$

can be calculated with the aid of the irreducible tensor operator technique;^{35–37} this matrix is given in Appendix I where the basis $|(S_{12})SM\rangle$ is used. It should be noted that the normal part of the AS exchange operates only within four $(S_{12})S = (0)1/2, (1)1/2$ low-lying states, whereas the in-plane part of AS exchange leads only to a mixing of the $S = 1/2$ and $3/2$ levels. Later on we will demonstrate that because of this circumstance these two parts of the AS exchange have different physical consequences in the field dependence of the magnetization.

3. Zeeman Levels in Perpendicular Field

A discussion of the symmetry properties of the Hamiltonian $H_0 + H_{AS}$ and the zero-field splitting has been recently given in our article.²⁸ In absence of the field, the system possesses actually axial symmetry, and the full pattern was shown to consist of four Kramers doublets, of which two originate from the accidentally degenerate levels $(S_{12})S = (0)1/2, (1)1/2$ and two from the excited $S = 3/2$ level. In the parallel magnetic field ($\mathbf{H} \parallel C_3$ axis), the axial symmetry is preserved, which allows the exact analytical solution for the Zeeman energy levels to be found, providing an arbitrary interrelation between all parameters of the system.

The low-temperature single-crystal magnetization experiments that will be discussed in this article are performed in the perpendicular ($\mathbf{H} \perp C_3$ axis) field. Under this condition, the axial symmetry is broken, and in general, the numerical analysis is required. Nevertheless, in the important particular case when only the normal contribution to the AS exchange is taken into account ($D_n \neq 0, D_l = D_t = 0$) the special symmetry properties of the matrix of AS exchange (that will not be discussed in this article) do allow the exact roots of the energy matrix to be found in the relevant particular case of perpendicular field ($\mathbf{H} \perp C_3$)

$$\begin{aligned} \epsilon_1 = \epsilon_3 &= -\frac{3}{2}J - \frac{1}{2}\sqrt{(g\beta H)^2 + 3D_n^2} \\ \epsilon_2 = \epsilon_4 &= -\frac{3}{2}J + \frac{1}{2}\sqrt{(g\beta H)^2 + 3D_n^2} \\ \epsilon_{5,6} &= \frac{3}{2}J \mp \frac{1}{2}g\beta H \\ \epsilon_{7,8} &= \frac{3}{2}J \mp \frac{3}{2}g\beta H \end{aligned} \quad (5)$$

Throughout the paper we are dealing with the perpendicular field; thus in eq 5 and in the subsequent expressions,

- (35) Varshalovich, D. A.; Moskalev, A. N.; Khersonskii, V. K. *Quantum Theory of Angular Momentum*; World Scientific: Singapore, 1988.
 (36) Bencini, A.; Gatteschi, D. *Electron Paramagnetic Resonance of Exchange Coupled Systems*; Springer-Verlag: New York, 1990.
 (37) Tsukerblat, B. S. *Group Theory in Chemistry and Spectroscopy*; Academic Press: London, 1994.

H is the field in any direction in the plane, say $H = H_x$, and correspondingly, the g factor is $g \equiv g_{\perp}$. The $\epsilon_i(H)$ levels with $i = 1, 2, 3, 4$ are related to $S = 1/2$, while those with $i = 5, 6, 7, 8$ are the numbers of Zeeman sublevels for $S = 3/2$ (with $M = 1/2$ and $M = 3/2$) as shown in Figure 4a in which the simplest case of the isotropic model is illustrated. The energy pattern for the case $D_n \neq 0, D_l = D_t = 0$ (eq 5) is shown in Figure 4b. Since the normal part of the AS exchange does not mix different spin states, the assignment of the levels to a specific full spin is valid also in this case. Three peculiarities of the energy pattern that are closely related to the magnetic behavior should be noted.

(1) The ground state involving two degenerate $S = 1/2$ levels shows zero-field splitting into two Kramers doublets separated by the gap $\Delta = \sqrt{3} D_n$ (see refs 14 and 18).

(2) At low fields, $g\beta H \leq \Delta$, the Zeeman energies are double degenerate and show quadratic dependence on the field like in a Van Vleck paramagnet

$$\begin{aligned}\epsilon_1 &= \epsilon_3 = -\sqrt{3}D_n/2 - (g\beta H)^2/4\sqrt{3}D_n \\ \epsilon_2 &= \epsilon_4 = -\sqrt{3}D_n/2 + (g\beta H)^2/4\sqrt{3}D_n\end{aligned}\quad (6)$$

This behavior is drastically different from that in the isotropic model and from the linear magnetic dependence in parallel field²⁸ and can be considered as a reduction of Zeeman interaction at the low perpendicular field by the normal AS exchange (see ref 14 and references therein). It is evident that the magnetic moments associated with the ground state are strongly reduced at low fields (all directions in the plane are hard axes of magnetization).

(3) The magnetic sublevels arising from $S = 3/2$ ($M = -1/2$ and $M = -3/2$) cross the sublevels belonging to $S = 1/2$ spin levels; no avoided crossing points are observed. At high perpendicular field (two first terms of the series), the Zeeman levels $\epsilon_1(H) = \epsilon_3(H)$ and $\epsilon_2(H) = \epsilon_4(H)$ again exhibit the linear magnetic dependence

$$\begin{aligned}\epsilon_1(H) &= \epsilon_3(H) = -\frac{3}{2}J - \frac{3D_n^2}{g\beta H} - \frac{1}{2}g\beta H \\ \epsilon_2(H) &= \epsilon_4(H) = -\frac{3}{2}J + \frac{3D_n^2}{g\beta H} + \frac{1}{2}g\beta H\end{aligned}\quad (7)$$

One can see that a strong perpendicular field restores linear Zeeman splitting but without zero-field splitting so that the perpendicular field reduces the normal part of AS coupling. The remaining (i.e., reduced) part of the AS exchange proves to be $6D_n^2/g\beta H$ and rapidly vanishes with the increase of the field. In the limit of the strong field, we obtain double-degenerate Zeeman levels ($\epsilon_1 = \epsilon_3$ and $\epsilon_2 = \epsilon_4$) that correspond to the in-plane disposition of the axis of quantization.

When the AS exchange in the most general form compatible with the trigonal symmetry is involved ($D_n \neq 0, D_l \neq 0, D_t \neq 0$), the energy pattern shows new peculiarities (Figure 4c). The low field part of the spectrum is not affected by the in-plane part of AS exchange and is very close both qualitatively and quantitatively to that in Figure 4b. This is because the in-plane part of AS exchange is not operative within the ground manifold and the effect of $S = 1/2$ and

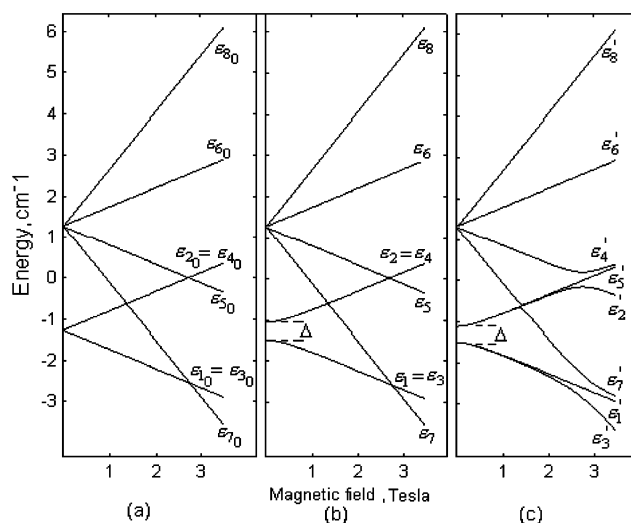


Figure 4. Energy pattern of the triangular vanadium unit in the magnetic field applied in the plane ($\mathbf{H} \perp C_3$), $J = 0.847 \text{ cm}^{-1}$, $g = 2$: (a) $D_n = 0, D_l = D_t = 0$; (b) $D_n = 0.3J, D_l = D_t = 0$; (c) $D_n = 0.3J, D_l = D_t = 0.6J$.

$S = 3/2$ mixing is small at low fields because of the large gap $3J \gg |D_{\perp}|$. The in-plane part of the AS exchange results in the zero-field splitting of the $S = 3/2$ level that is a second-order effect and cannot be seen in the scale of Figure 4. At the same time, in the vicinity of the crossing points, the effect of the normal AS exchange is negligible but the in-plane part of AS exchange acts as a first-order perturbation²⁸ giving rise to the avoided crossings in the ground and excited states as shown in Figure 4c.

For the evaluation of the low-temperature part of the magnetization, only the low-lying levels are important. Let us note that at low fields, far from the anticrossing region, the energies can be well described by eq 5 in the general case of AS exchange, although they are deduced for a particular model when $D_n \neq 0, D_l = D_t = 0$. To obtain three closely spaced low-lying levels as functions of the magnetic field in the region of anticrossing, we will use the perturbation theory taking the in-plane part of AS exchange as the perturbation and the spin basis formed by three eigenfunctions of $H_0 + g_{\perp} \beta (H_x S_x + H_y S_y)$ whose eigen-values have their crossing point at $g\beta H = 3J$, namely, $|0\rangle(1/2, -1/2), |1\rangle(1/2, -1/2), |1\rangle(3/2, -3/2)$ which are referred to the quantization axis being in the plane of the triangle. The linear behavior of these levels corresponding to a new axis of quantization can be seen from Figure 4a and b. The functions so far described can be interrelated to the initial basis in the adapted molecular frame. The basis and the 3×3 matrix of the full Hamiltonian in this basis are given in Appendix II. The corresponding secular equation can be solved because of the presence of an additional symmetry that will not be discussed in this short article. The following expressions for the energy levels $\epsilon'_i(H)$ found in this region of the field are

$$\epsilon'_1(H) = -\frac{3}{2}J - \frac{1}{2}g\beta H \quad (8)$$

$$\epsilon'_3(H) = -g\beta H - \frac{1}{8}\sqrt{(4g\beta H - 12J)^2 + 18D_{\perp}^2} \quad (9)$$

$$\epsilon'_7(H) = -g\beta H + \frac{1}{8}\sqrt{(4g\beta H - 12J)^2 + 18D_{\perp}^2} \quad (10)$$

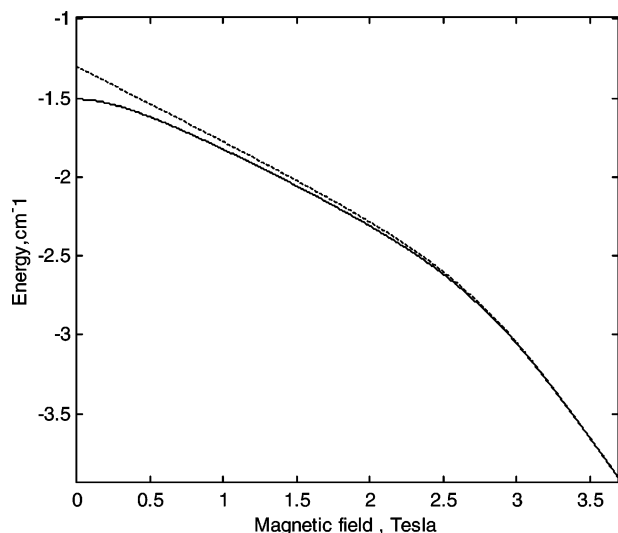


Figure 5. Ground-state level of the V_{15} cluster (solid line) and numerical calculation (dashed line according to eq 10): $J = 0.847 \text{ cm}^{-1}$, $D_n = 0.3J$, $D_{\perp} = 0.6J$.

where the notation $D_{\perp}^2 = D_r^2 + D_l^2$ is introduced. It should be noted that these approximate expressions illustrate a general statement that there are only two effective parameters of AS exchange, namely, D_n and D_{\perp} , and not three as initially introduced. Figure 5 illustrates the comparison of the ground energy level versus the field calculated using eq 9 with the exact numerical solution. One can see that although eqs 8–10 are based on the perturbation theory they provide a rather good accuracy not only in the vicinity of the anticrossing point $g\beta H = 3J$ but also in a wide region of the field with the exception of the low-field region $g\beta H \leq \Delta$, in which the normal part of the AS exchange plays a predominant role (see Figure 4b and c), and the restricted basis so far used proves to be irrelevant. In this region of the field, the low-lying energy levels are well reproduced by eq 5.

4. Temperature and Field Dependence of Magnetization: Effects of AS Exchange

Molecular magnetization in the direction $\alpha = x, y, z$ as a function of the field and temperature is defined by the conventional expression^{33,38}

$$\mu_{\alpha}(H_{\alpha}, T) = \frac{\sum_n \left(-\frac{\partial \epsilon_n}{\partial H_{\alpha}} \right) \exp\left(-\frac{\epsilon_n}{kT}\right)}{\sum_n \exp\left(-\frac{\epsilon_n}{kT}\right)} \quad (11)$$

Before we discuss the experimental data on the V_{15} cluster, let us consider some general features of the field dependence of magnetization related to the AS exchange by plotting the results of sample calculations. From this point of view, the most spectacular is the low-temperature limit for which, with the aid of eqs 6 and 9, one can find the following expressions

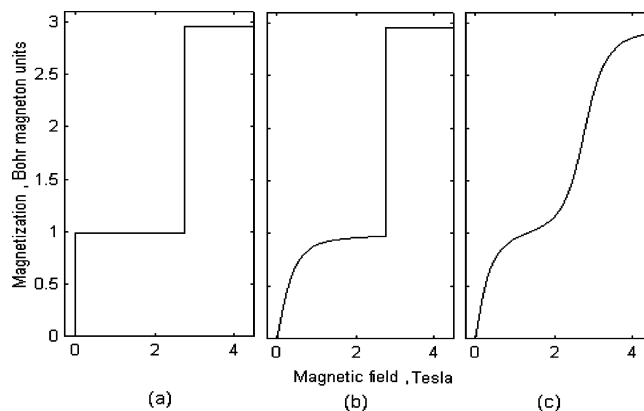


Figure 6. Magnetization at $T = 0 \text{ K}$ in the perpendicular field for the cases: (a) $J = 0.847 \text{ cm}^{-1}$, $D_n = 0$, $D_{\perp} = 0$; (b) $J = 0.847 \text{ cm}^{-1}$, $D_n = 0.3J$, $D_{\perp} = 0$; (c) $J = 0.847 \text{ cm}^{-1}$, $D_n = 0.3J$, $D_{\perp} = 0.6J$.

for magnetization in the perpendicular field (per molecule) that work well at low field (eq 12) and high field (eq 13) in the range of anticrossing of the low lying levels.

$$\mu(H) = \frac{g^2 \beta^2 H}{2\sqrt{3D_n^2 + g^2 \beta^2 H^2}} \quad (12)$$

$$\mu(H) = g\beta + \frac{2g\beta(g\beta H - 3J)}{\sqrt{16(g\beta H - 3J)^2 + 18D_{\perp}^2}} \quad (13)$$

Because of the effect of the reduction of the Zeeman interaction at low field by the normal AS exchange, the magnetization in this region of the field proves to be induced by the field as follows from eq 12. In fact these simple equations provide high precision in the full range of the field as follows from the comparison with the results of exact calculation. In Figure 6 (using the parameter of the isotropic exchange $J = 0.847 \text{ cm}^{-1}$ reported in ref 29), we show the field dependence of magnetization at $T = 0$ within the triangular model. We do not have at our disposal clearly defined AS exchange parameters for the V_{15} cluster, especially the interrelation between normal and in-plane parts. Under these circumstances, to make the illustration more clear, we artificially increased the parameters of the AS exchange.

Figure 6a shows the $\mu(H)$ dependence at $T = 0$ in the framework of the isotropic model when the magnetization exhibits two sharp nonbroadened steps, one at zero field and the second at $H = 3J/g\beta$ field, where the level with $S = 3/2$, $M = -3/2$ crosses the degenerate pair of levels ($S_{12} = 0$ and $S_{12} = 1$) $S = 1/2$, $M = -1/2$, so that the $S = 3/2$ level becomes favorable against $S = 1/2$; this can be clearly seen in Figure 6a. In Figure 6b, the effect of the normal part of the AS exchange is illustrated. As one can see, the normal part of the AS exchange results in the broadening of the low-field step in $\mu(H)$, while the high-field step remains nonbroadened. The broadening of the first step is closely related to the magnetic anisotropy of the AS exchange that gives rise to a quadratic Zeeman effect in the low perpendicular field (see Figure 4b). It can be said that the normal part of

(38) Kahn, O. *Molecular Magnetism*; VCH: New York, 1993.

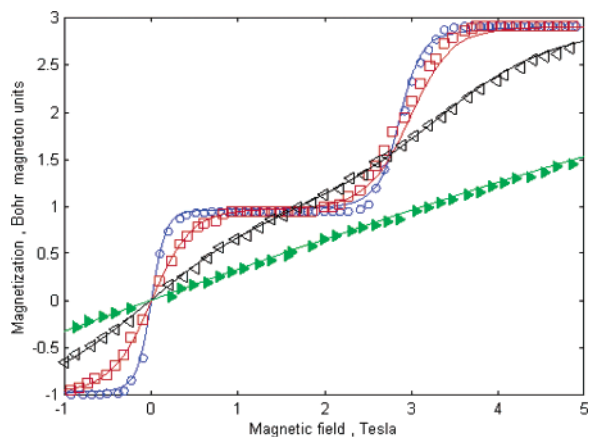


Figure 7. Experimental data (from ref 29) and theoretical curves of static magnetization calculated with account for the isotropic and AS exchange interactions ($\mathbf{H} \perp C_3$). Experimental data: circles, $T = 0.1$ K; squares, $T = 0.3$ K; unfilled triangles, $T = 0.9$ K; filled triangles, $T = 4.2$ K. Solid lines represent the calculated curves with the best fit of the parameters (see text).

AS exchange reduces the perpendicular magnetization at low field and allows only second-order magnetic splitting and Van Vleck paramagnetism. Since the magnetization is induced by the field and does depend on the field even at $T = 0$, the jump of $\mu(H)$ acquires a peculiar shape (Figure 6b). At the same time, the normal AS exchange leaves the exact crossing of $S = 3/2$, $M = -3/2$ level with the lowest component of $S = 1/2$ that results in absence of the broadening of the high-field step (Figure 6b). Finally, when both the normal and in-plane parts of the AS exchange are taken into account, we obtain broadening of both steps (Figure 6c). Now the anticrossing in the region $H = 3J/g\beta$ appears because of the coupling of $S = 1/2$, $M = -1/2$ and $S = 3/2$, $M = -3/2$ levels through in-plane AS exchange that obviously gives rise to a smoothed switch from $S = 1/2$ to $3/2$, as shown in Figure 6c.

5. Temperature and Field Dependence of Magnetization of V_{15} Cluster

The low-temperature ($T = 0.1, 0.3, 0.9, 4.2$ K) adiabatic magnetization experiments of V_{15} single crystals have been reported in ref 29. The adiabatic magnetization versus field applied in the plane of the V_3 triangle ($\mathbf{H} \perp C_3$) exhibits steps whose broadening and shapes are temperature dependent (Figure 7). Analysis of the experimental data in ref 29 has been performed in the framework of isotropic exchange model, eq 1, and also in a more general model that takes into account second-order anisotropic contributions such as axial quadrupolar anisotropy ($J_{xx} = J_{yy} \neq J_{zz}$). Agreement between the calculated curves and the experimental magnetization data proved to be quite good for $T = 0.9$ and 4.2 K, but the model fails to provide a fit to the low-temperature data. In view of this, the AS exchange has been mentioned in ref 29 as a possible origin of the broadening of the steps in the magnetization curve.

Modeling studies of the magnetization curves at different temperatures and the simple expressions in refs 12 and 13

show that the low-temperature behavior of the magnetization versus field is most sensitive to the AS exchange, while at higher temperature ($T > 2$ K), the effect of the smoothing of the steps caused by population of the excited levels dominates. To avoid artificial fitting, we adopt the following initial set of parameters: $J = -0.847$ cm^{-1} , $g = 1.952$, and $D_{\perp} = 0.22$ cm^{-1} . This set of parameters gives the best fit to the experimental data at very low temperature (0.1 K) in the shape of the high-field step at $H \approx 2.8$ tesla, corresponding to the $S = 3/2$ to $S = 1/2$ crossing region (eq 13). On the basis of the zero-field splitting value of the degenerate spin doublets, $\Delta = 0.14$ cm^{-1} , found from inelastic neutron scattering experiments^{39,40} the expression containing second-order correction with respect to the in-plane part of AS exchange, $\Delta = \sqrt{3} D_n - D_{\perp}^2/8J$, was used.²⁸ Taking this into account, we can get a reasonable initial value of $D_n = 0.0851$ cm^{-1} . The fit is reached by minimization of the mean square error (hereafter MSE) defined as

$$\text{MSE} = (1/N) \sum_i^N (\mu_{\text{theor}}(H_i) - \mu_{\text{exp}}(H_i))^2 \quad (14)$$

The best-fit procedure gives the following set of parameters: $J = -0.855$ cm^{-1} , $g = 1.94$, $D_{\perp} = 0.238$ cm^{-1} , and $D_n = 0.054$ cm^{-1} . The parameter J found from the best fit is very close to that estimated in ref 29. It should be noted that in-plane parameter D_{\perp} brings a dominating contribution to the overall AS exchange. This parameter is directly responsible for the behavior of the levels in the anticrossing region $H \approx 2.8$ tesla. Figure 7 shows that the model that includes AS exchange interaction gives the perfect field-dependence magnetization fit in the whole range of fields for all temperatures including extremely low temperature.

The least MSE value (in μ_B^2) calculated for the whole set of $\mu(H)$ curves is found to be 2.3×10^{-3} . The MSE values for the curves corresponding to different temperatures are the following: 1.7×10^{-3} ($T = 0.1$ K), 5.1×10^{-3} ($T = 0.3$ K), 5.61×10^{-4} ($T = 0.9$ K), and 6.97×10^{-4} ($T = 4.2$ K). This shows that the best-quality fit is reached at the highest temperature. In fact, the data at 4.2 K are only slightly affected by AS exchange so this fit is almost insensitive to the model. In fact, the best fit for 4.2 K in the isotropic model (at $J = 0.86$ cm^{-1} , $g = 1.945$) can be obtained with $\text{MSE} = 8.38 \times 10^{-4}$ which does not exceed significantly the corresponding value (6.97×10^{-4}) in the model with the account for AS exchange. The best-fit parameters J and g are very close in both models, which demonstrates the low sensitivity of the theoretical curves to the AS exchange at 4.2 K. On the contrary, the data at 0.1 K cannot be fitted within the isotropic model (mentioned already in²⁹) but are fitted perfectly with the significant reduction of MSE from 6.3×10^{-3} to 1.7×10^{-3} when AS exchange is taken into account.

(39) Chaboussant, G.; Basler, R.; Sieber, A.; Ochsenein, S. T.; Desmedt, A.; Lechner, R. E.; Telling, M. T. F.; Kögerler, P.; Müller, A.; Güdel, H.-U. *Europhys. Lett.* **2002**, *59* (2), 291.

(40) Chaboussant, G.; Ochsenein, S. T.; Sieber, A.; Güdel, H.-U.; Mutka, H.; Müller, A.; Barbara, B. *Europhys. Lett.* **2004**, *66* (3), 423.

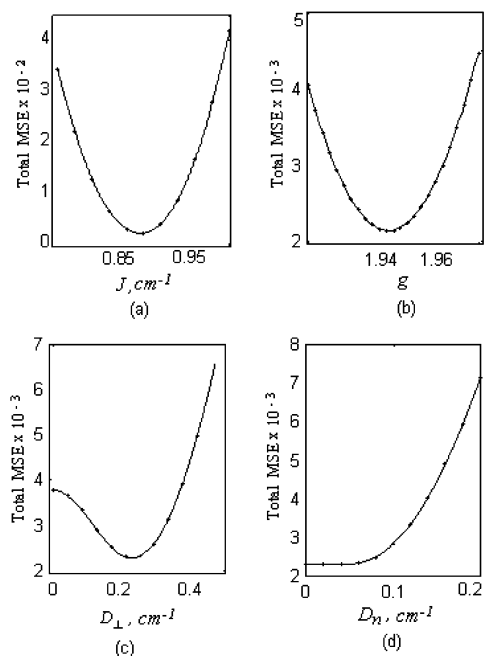


Figure 8. Total mean square errors as functions of the parameters J (a), g (b), D_{\perp} (c), and D_n (d).

The reliability of the fit can be illustrated by plotting the total MSE versus the best-fit parameters near the least MSE point. These plots are shown in Figure 8 for each parameter provided that the remaining parameters are fixed. One can see that the fit is stable for the parameters J , g , and D_{\perp} , but however, it is less stable with respect to D_n . To determine this parameter more accurately, one needs low-field data at ultralow temperatures and additional data like EPR at low frequencies. In particular, one can expect that, in line of the general Moria's theory,¹³ the parameters D_n and D_{\perp} can be interrelated with $(\Delta g_{\parallel}/g)J$ and $(\Delta g_{\perp}/g)J$ correspondingly (this has been mentioned by a referee of this paper). To extract more information, more detailed EPR measurements would be useful.

Conclusion

We have analyzed the experimental data of the low-temperature adiabatic magnetization of the nanoscopic low-spin cluster anion present in $\text{K}_6[\text{V}^{\text{IV}}_{15}\text{As}_6\text{O}_{42}(\text{H}_2\text{O})] \cdot 8\text{H}_2\text{O}$ as a function of applied field and temperature. The three-spin model of V_{15} was employed which includes isotropic exchange interaction and antisymmetric AS exchange in the most general form compatible with the trigonal symmetry of the system. It was shown that the AS exchange plays a crucial role in the understanding of the field and temperature dependence of the adiabatic magnetization of V_{15} . Although the initial Hamiltonian of the AS exchange involves three coupling constants, only two effective parameters are responsible for the physical manifestations of AS exchange. Furthermore, it was demonstrated that the orientation of the AS exchange vector, not only its absolute value, plays a special physical role in the magnetic behavior of spin-frustrated systems. In fact, the normal part of the AS exchange affects the low-field part of the magnetization curve when the field

is applied in the plane of the V_3 triangle. At the same time, the in-plane components of AS exchange give rise to a peculiar shape of magnetization versus field in the vicinity of the crossing point of the magnetic sublevels belonging to $S = 1/2$ and $3/2$ levels. The influence of the AS exchange is most pronounced at very low temperature ($T = 0.1$ K).

It was possible to reach a perfect fit to the experimental data on the adiabatic magnetization versus applied in-plane field in the whole temperature range including extremely low temperature and, for the first time, to estimate precisely two components of the AS vector coupling constant, namely, the effective in-plane component, D_{\perp} , and the perpendicular part, D_n . Furthermore it can be concluded that we understand more about the physical contents of the concept of spin frustration and about frustrated systems integrated in complex systems. Therefore, we intend to extend this to other complex systems, for example, where frustrated systems are interacting as in $\{\text{Mo}_{57}\}\{\text{V}_3\}_2$ ^{34a} (see also the Introduction). We left out of the present discussion the question of the vibronic Jahn–Teller interaction that is inherently related to the orbital degeneracy and spin frustration. This interaction is estimated to be negligible for the V_{15} cluster but can play an essential role in the magnetic behavior of spin-frustrated systems if the vibronic interaction is comparable with the AS exchange.⁴¹

Acknowledgment. Financial support from the German–Israeli Foundation (GIF) for Scientific Research & Development (grcanc G-775-19.10/2003) is gratefully acknowledged. A.M. thanks also the Deutsche Forschungsgemeinschaft, the Fonds der Chemischen Industrie, the European Union, and the Volkswagenstiftung.

Appendix I. Matrix Representation of the Full Hamiltonian

One can express the Hamiltonian, eq 3, in terms of the irreducible tensor operators (ITO) with the aid of the well-known^{18,33,35–37} interrelations between the spherical components ($q = 0, \pm 1$) of the vector product and the first rank irreducible tensor product

$$[\mathbf{S}_i \times \mathbf{S}_j]_q = -i\sqrt{2}\{S_1^i \times S_1^j\}_{1,q} \quad (\text{I.1})$$

where S_{1q}^i ($i = 1, 2, 3$) is the spin tensor (first-order ITO) relating to the site i and $\{S_1^i \times S_1^j\}_{k,q}$ is the component q of the tensor product of the rank k . Straightforward calculation leads to the following Hamiltonian of AS the exchange expressed in terms of ITO

$$\begin{aligned} H_{\text{AS}} = & -i\sqrt{2}D_n(\{S_1^1 \times S_1^2\}_{1,0} + \{S_1^2 \times S_1^3\}_{1,0} + \{S_1^3 \times \\ & S_1^1\}_{1,0}) + (D_t + iD_{\parallel})\{S_1^1 \times S_1^2\}_{1,1} + (D_t - iD_{\parallel})\{S_1^1 \times \\ & S_1^2\}_{1,-1} + \omega^*(D_t + iD_{\parallel})\{S_1^2 \times S_1^3\}_{1,1} + \omega(D_t - iD_{\parallel})\{S_1^2 \times \\ & S_1^3\}_{1,-1} + \omega(D_t + iD_{\parallel})\{S_1^3 \times S_1^1\}_{1,1} + \omega^*(D_t - iD_{\parallel})\{S_1^3 \times \\ & S_1^1\}_{1,-1} \quad (\text{I.2}) \end{aligned}$$

(41) Tsukerblat, B.; Tarantul, A.; Müller, A. *J. Mol. Struct.* In press.

where $\omega = \exp(2\pi i/3)$. This is the most common expression for the AS exchange Hamiltonian compatible with the trigonal symmetry. The matrix elements of the pairwise AS exchange interactions in the triangle within the $|(S_{12})SM\rangle$ basis can be calculated for an arbitrary set of S_1, S_2, S_3 in a general way with the use of the ITO approach (see refs 18, 33, 35–37). The final result for the matrix elements of the $S_i = 1/2$ triangle are

$$\begin{aligned} \langle (S_{12})SM | \{S_1^1 \times S_1^2\}_{1,q} | (S'_{12})S'M' \rangle = & \\ & -\frac{3\sqrt{3}}{2}(-1)^{1/2+S+S'+2S_{12}-M} \begin{pmatrix} S & 1 & S' \\ -M & q & M' \end{pmatrix} \times \\ & \sqrt{[S][S'] [S_{12}][S'_{12}]} (S'_{12} - S_{12})(S_{12} + S'_{12} + 1) \\ & \begin{Bmatrix} S & S_{12} & 1/2 \\ S'_{12} & S' & 1 \end{Bmatrix} \begin{Bmatrix} 1/2 & S_{12} & 1/2 \\ S'_{12} & 1/2 & 1 \end{Bmatrix} \langle (S_{12})SM | \{S_1^2 \times S_1^3\}_{1,q} | \\ & (S'_{12})S'M' \rangle = \frac{\sqrt{3}}{4}(-1)^{3S+S'+2S_{12}+2S'_{12}+3/2-M} \begin{pmatrix} S & 1 & S' \\ -M & q & M' \end{pmatrix} \times \\ & \sqrt{[S][S'] [S_{12}][S'_{12}]} [(S_{12} - S'_{12})(S_{12} + S'_{12} + 1) - (S - S')] \\ & (S + S' + 1) \times \begin{Bmatrix} S'_{12} & 1/2 & 1/2 \\ 1/2 & S_{12} & 1 \end{Bmatrix} \begin{Bmatrix} S_{12} & S & 1/2 \\ S' & S'_{12} & 1 \end{Bmatrix} \langle (S_{12})SM | \\ & \{S_1^3 \times S_1^1\}_{1,q} | (S'_{12})S'M' \rangle = \frac{\sqrt{3}}{4}(-1)^{3S+S'+S_{12}+3S'_{12}+3/2-M} \\ & \begin{pmatrix} S & 1 & S' \\ -M & q & M' \end{pmatrix} \sqrt{[S][S'] [S_{12}][S'_{12}]} [(S_{12} - S'_{12})(S_{12} + S'_{12} + \\ & 1) - (S - S')(S + S' + 1)] \times \begin{Bmatrix} S_{12} & 1/2 & 1/2 \\ 1/2 & S'_{12} & 1 \end{Bmatrix} \\ & \begin{Bmatrix} S_{12} & S & 1/2 \\ S' & S'_{12} & 1 \end{Bmatrix} \quad (\text{I.3}) \end{aligned}$$

where the conventionally accepted notations for the $3j$ and $6j$ symbols are used and $[S] = 2S + 1$.

After substitution of the numerical values of the $3j$ and $6j$ symbols,³⁵ one obtains the matrix of the full Hamiltonian $H_0 + H_{AS} + H_{Zeem}$ in the $|(S_{12})SM\rangle$ basis as follows:

$$\begin{bmatrix} -\frac{3}{2}J + \frac{1}{2}h_z & \frac{1}{\sqrt{2}}h_- & -i\frac{\sqrt{3}}{2}D_n & 0 & \frac{3}{4}iD_+ & 0 & \frac{\sqrt{3}}{4}iD_- & 0 \\ -\frac{1}{\sqrt{2}}h_+ & -\frac{3}{2}J - \frac{1}{2}h_z & 0 & i\frac{\sqrt{3}}{2}D_n & 0 & \frac{\sqrt{3}}{4}iD_+ & 0 & \frac{3}{4}iD_- \\ i\frac{\sqrt{3}}{2}D_n & 0 & -\frac{3}{2}J + \frac{1}{2}h_z & \frac{1}{\sqrt{2}}h_- & -\frac{3}{4}D_+ & 0 & \frac{\sqrt{3}}{4}D_- & 0 \\ 0 & -i\frac{\sqrt{3}}{2}D_n & -\frac{1}{\sqrt{2}}h_+ & -\frac{3}{2}J - \frac{1}{2}h_z & 0 & -\frac{\sqrt{3}}{4}D_+ & 0 & \frac{3}{4}D_- \\ \frac{3}{4}iD_- & 0 & \frac{3}{4}D_- & 0 & \frac{3}{2}J + \frac{3}{2}h_z & \sqrt{\frac{3}{2}}h_- & 0 & 0 \\ 0 & \frac{\sqrt{3}}{4}iD_- & 0 & \frac{\sqrt{3}}{4}D_- & -\sqrt{\frac{3}{2}}h_+ & \frac{3}{2}J + \frac{1}{2}h_z & \sqrt{2}h_- & 0 \\ \frac{\sqrt{3}}{4}iD_+ & 0 & -\frac{\sqrt{3}}{4}D_+ & 0 & 0 & -\sqrt{2}h_+ & \frac{3}{2}J - \frac{1}{2}h_z & \sqrt{\frac{3}{2}}h_- \\ 0 & \frac{3}{4}iD_+ & 0 & -\frac{3}{4}D_+ & 0 & 0 & -\sqrt{\frac{3}{2}}h_+ & \frac{3}{2}J - \frac{3}{2}h_z \end{bmatrix}$$

In the matrix representation the following order of the basis spin-functions is assumed

$$|(0)\frac{1}{2}, \frac{1}{2}\rangle, |(0)\frac{1}{2}, -\frac{1}{2}\rangle, |(1)\frac{1}{2}, \frac{1}{2}\rangle, |(1)\frac{1}{2}, -\frac{1}{2}\rangle, |(1)\frac{3}{2}, \frac{3}{2}\rangle, |(1)\frac{3}{2}, \frac{1}{2}\rangle, |(1)\frac{3}{2}, -\frac{1}{2}\rangle, |(1)\frac{3}{2}, -\frac{3}{2}\rangle$$

We use the notations $D_{\pm} = \mp \frac{1}{\sqrt{2}}(D_l \pm iD_t)$, which are the cyclic components (defined in ref 35) of the AS exchange vector, $h_{\pm} = \mp \frac{g_{\perp}\beta}{\sqrt{2}}(H_x \pm iH_y)$, and $h_z = g_{\parallel}\beta H_z$.

Appendix II. Matrix of the Perpendicular Part of the AS Exchange Operator and Zeeman Interaction in the Restricted Basis

The unperturbed Hamiltonian, $H_0 + g_{\perp}\beta(H_x S_x + H_y S_y)$, that includes the isotropic exchange and perpendicular part of the Zeeman interaction has the following eigenvectors that correspond to the low-lying crossing levels (Figure 4a, 4b):

$$\begin{aligned} |(1)\frac{3}{2}, M_{\perp} = -\frac{3}{2}\rangle &= \frac{\sqrt{2}}{4}|(1)\frac{3}{2}, \frac{3}{2}\rangle - \frac{\sqrt{6}}{4}|(1)\frac{3}{2}, \frac{1}{2}\rangle + \frac{\sqrt{6}}{4}|(1)\frac{3}{2}, -\frac{1}{2}\rangle - \frac{\sqrt{2}}{4}|(1)\frac{3}{2}, -\frac{3}{2}\rangle \\ |(0)\frac{1}{2}, M_{\perp} = -\frac{1}{2}\rangle &= -\frac{\sqrt{2}}{2}|(0)\frac{1}{2}, \frac{1}{2}\rangle + \frac{\sqrt{2}}{2}|(0)\frac{1}{2}, -\frac{1}{2}\rangle \\ |(1)\frac{1}{2}, M_{\perp} = -\frac{1}{2}\rangle &= -\frac{\sqrt{2}}{2}|(1)\frac{1}{2}, \frac{1}{2}\rangle + \frac{\sqrt{2}}{2}|(1)\frac{1}{2}, -\frac{1}{2}\rangle \quad (\text{II.1}) \end{aligned}$$

These spin functions (left-hand side of eq II.1) are enumerated by the full spin, S , and intermediate spin quantum number, S_{12} , and correspond to the spin projections

$$M_{\perp} = -\frac{3}{2}(S_{12} = 1, S = \frac{3}{2})$$

and

$$M_{\perp} = -\frac{1}{2}(S_{12} = 1, S = \frac{1}{2} \text{ and } S_{12} = 0, S = \frac{1}{2})$$

while the quantization axis is aligned in the plane of the

Static Magnetization of V_{15} Cluster

triangle (symbolized by the sign \triangle), in other words, coincides with the direction of H for a strong field. The eigenvectors correspond to the following eigen values in which H is the field in the arbitrary direction in the plane

$$\begin{aligned} \epsilon\left(1\frac{3}{2}, M_{\perp} = -\frac{3}{2}\right) &= \frac{3}{2}J - \frac{3}{2}g\beta H, \quad \epsilon\left(0\frac{1}{2}, M_{\perp} = -\frac{1}{2}\right) = \\ &= \epsilon\left(1\frac{1}{2}, M_{\perp} = -\frac{1}{2}\right) = -\frac{3}{2}J - \frac{1}{2}g\beta H \quad (\text{II.2}) \end{aligned}$$

Since the AS exchange is not included in the unperturbed Hamiltonian the $S = 1/2$ levels form degenerate pairs. Using the eigen-vectors given in eq II.1 and the matrix of the AS exchange and Zeeman interaction from Appendix I as a basis,

one can find the following 3×3 matrix of the AS exchange in which the Zeeman part is diagonal:

$$\begin{pmatrix} \frac{3}{2}(J - g\beta H) & -\frac{3D_t}{4\sqrt{2}} & -\frac{3D_t}{4\sqrt{2}} \\ -\frac{3D_t}{4\sqrt{2}} & \frac{1}{2}(-3J - g\beta H) & 0 \\ -\frac{3D_t}{4\sqrt{2}} & 0 & \frac{1}{2}(-3J - g\beta H) \end{pmatrix} \quad (\text{II.3})$$

The eigenvalues of this matrix are given in eqs 8–10.

IC061394J